Available online at www.sciencedirect.com
SCIENCE DIRECT®
Surface Science 532–535 (2003) 317–323
SURFACE SCIENCE
www.elsevier.com/locate/susc

Formation of aluminum nanodot array by combination of nanoindentation and anodic oxidation of aluminum

Shoso Shingubara *, Yusuhiko Murakami, Kazunori Morimoto, Takayuki Takahagi

Graduate School of Advanced Sciences and Matters, Hiroshima University, 1-3-1 Kagamiyama, Higashi-Hiroshima 739-8530, Japan

Abstract

Porous alumina films formed by aluminum anodic oxidation have been intensively studied to use them as molds to form nanowires or dots. Recently we established the formation of porous alumina on solid substrates such as Si, and found a formation of an ordered aluminum hexagonal dot array after finishing of anodic oxidation on a SiO_2 substrate. We investigated AFM nanoindentation to control the initial position of nanoholes during anodic oxidation, in order to realize nanoholes and dots with various sizes and densities. Arrays of nanoholes with a nearest neighbor distance from 50 to 120 nm were successfully formed. Al dot tetragonal and hexagonal arrays were formed after selective wet chemical etching of porous alumina film. Electron transport through Al nanodots array at low temperature exhibited a non-linear characteristic with a suppression of current around zero bias, which strongly suggests existence of Coulomb blockade.

Keywords: Electrochemical methods; Electrical transport measurements; Aluminum; Aluminum oxide; Electrical transport (conductivity, resistivity, mobility, etc.); Self-assembly; Surface structure, morphology, roughness, and topography; Solid–liquid interfaces

1. Introduction

Porous alumina films formed by anodic oxidation of aluminum (Al) have been intensively studied for use as molds to form nanowires or dots by depositing various metals or semiconductors in them, since highly ordered nanohole arrays can be formed [1–12]. By the use of oxalic acid, sulfuric acid, or phosphoric acid, trigonal lattices of alumina nanoholes with distances of several tens of nm can be formed under the self-organization conditions of anodic oxidation. We recently succeeded in forming an Al dot hexagonal array on a SiO_2/Si(1 0 0) substrate through adequate conditions of anodic oxidation and the subsequent selective removal of porous alumina film [13–15]. Al dots measuring a few tens of nm were formed at an interface between the porous alumina film and the SiO_2 film by a break-up of Al film due to completion of anodic oxidation. These Al dots are useful for application to quantum effect devices such as single electron memory nodes or quantum cellular automata devices based on tunneling phenomena within two-dimensional quantum dot

* Corresponding author. Address: Department of Electrical Engineering, Hiroshima University, 1-4-1 Kagamiyama, Higashi-Hiroshima 739-8527, Japan. Tel.: +81-824-24-7645; fax: +81-824-22-7195.
E-mail address: shingu@hiroshima-u.ac.jp (S. Shingubara).

0039-6028/03/$ - see front matter © 2003 Published by Elsevier Science B.V.
doi:10.1016/S0039-6028(03)00433-3

arrays [16]. However, the size and geometrical arrangement of the ordered porous alumina nanohole array are restricted by the self-organization conditions of each acid species. For example, the nearest neighbor distances of nanoholes at the self-organization condition are 475, 90 and 60 nm for phosphoric acid (anodization voltage $V_a = 195$ V) [10], oxalic acid ($V_a = 40$ V) [7,8], and sulfuric acid ($V_a = 28$ V) [9], respectively. Furthermore, the arrangement of nanoholes is limited to trigonal lattices only. It is desirable to form an ordered nanohole array with a desired dimension and geometry, and Masuda et al. proposed pretexturing of aluminum surface using SiC molds that had lithographically delineated periodic convexes [17,18].

In this study, at first, detail characterizations of Al dots formed on SiO_2/Si substrate were made by atomic force microscopy (AFM) and transmission electron microscopy (TEM) observations. Then a control of a geometrical arrangement of a nanohole array as well as Al dots by the use of AFM nanoindentation were investigated. We focused on the effect of indentation interval on a regularity of nanohole array in this experiment. Finally, electrical conduction characteristics between Al dots were examined by attaching electrodes using focused ion beam induced tungsten deposition.

2. Results and discussion

In order to form porous alumina film on SiO_2/Si substrate, we deposited pure aluminum (99.999%) film by sputtering on the substrate. The essential point to get well-ordered nanohole array for sputtered Al film by anodic oxidation is to keep aluminum surface flat. The regularity of nanohole arrangement is delicately dependent on the aluminum surface roughness, and usually regularity is poor when the surface roughness is large. For this reason, electropolishing with a diluted perchloric acid is carried out in the most cases of anodic oxidation for bulk Al. In the present study using sputtered Al films, it is difficult to deposit thick Al film to undergo electropolishing, hence we optimized sputtering conditions to keep surface as flat as can. The typical sputtering rate of Al is about 10–15 nm/min, and substrate was tightly attached to water-cooled copper block, and furthermore, sputtering was carried out by alternation of 1 min deposition and 1 min rest so as not to raise substrate temperature. By this method, aluminum film surface roughness could be controlled within 2 nm in root mean square roughness (RMS) even for Al films which thickness were larger than 10 μm.

When an anodic oxidation of Al film is carried out with the typical self-organization conditions of 40 V at 2 °C in 0.15 M oxalic acid solution, well-ordered nanohole array is obtained when Al film thickness is larger than 10 μm. By a so-called two step anodic oxidation in which a properly long first anodization and selective removal of porous alumina film were carried out, a well ordered nanohole array is formed in the second anodic oxidation [7]. Poly-crystalline domain structure of nanohole trigonal lattice is formed, and the domain size increases with an increase in the first step anodic oxidation time. It is not clear whether domain boundary corresponds to the crystalline grain boundary. The domain size might be limited by the grain size in the cases of self-organized formation of nanohole arrays.

When a long time anodic oxidation is carried out, most of the Al film is converted to porous alumina. We found a formation of Al dot at the interface between porous alumina and SiO_2. Initial sputtered Al thickness was 20 μm, and anodic oxidation was carried out with 40 V by 0.15 M oxalic acid. Cross-sectional views of Al dots are shown in Fig. 1. Scanning electron microscopy (SEM) micrographs of the nanohole bottoms shown in Fig. 1(a) and (b) were taken at different locations on the same sample formed by 10 h anodic oxidation. These micrograph was taken after cutting the Si substrate, and the Al cross-section was slightly elongated. In some areas, Al film was still continuous while periodic roughness reflecting hemispherical nanohole bottoms existed as Fig. 1(a). However, Al film broke-up to individual dots in other areas as seen in Fig. 1(b). A non-uniformity of the rate of anodic oxidation would be ascribed to distribution of electric field because electrode was contacted at the limited area of the Al surface. With an enough long anodic oxidation of 11 h, the entire Al dots were converted to

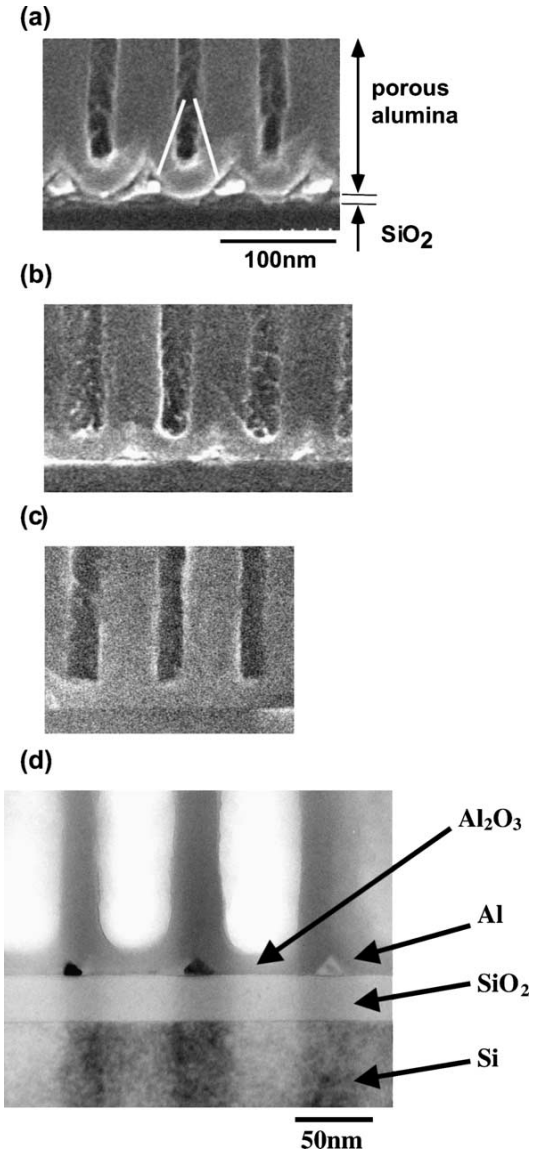

Fig. 1. Cross-sectional view of Al dots formed by anodic oxidation of sputtered Al film on SiO_2 (50 nm)/Si substrate. Initial sputtered Al thickness was 20 μm, and anodic oxidation was carried out with 40 V by 0.15 M oxalic acid. (a–c) SEM cross-sectional micrographs of the nanohole bottoms. (a and b) Observations at different locations on the same sample with 10 h anodic oxidation. (c) Sample with 11 h anodic oxidation. (d) Cross-sectional TEM micrograph of Al dots after 10.5 h anodic oxidation.

alumina as shown in Fig. 1(c). Thus anodic oxidation gradually proceeds even after breaking-up of Al film to dots, and this phenomena was supposed to be carried out by ionic conduction within anodic alumina film. A cross-sectional TEM micrograph of Al dots (Fig. 1d) clearly showed crystalline phase of Al dot.

AFM observations of the remaining Al after selective wet chemical etching of porous alumina using a mixture of chromic acid and phosphoric acid are shown in Fig. 2. The observed sample was formed by 10.5 h and 40 V anodic oxidation by 0.15 M oxalic acid with the initial Al thickness of 20 μm. It is clear that Al hexagonal nanodot array is formed on a flat surface of SiO_2. The diameter and height of the Al dots are 40 and 15 nm, respectively, and the nearest-neighbor distance of the Al dots is 65 nm. The diameter of the hexagon is equal to the cell size of the nanoholes. This is one typical example of Al dot array, however, there is a serious problem in realizing large area Al dot array because non-uniformities existed in the dot size as well as in the inter-dot spacing. They

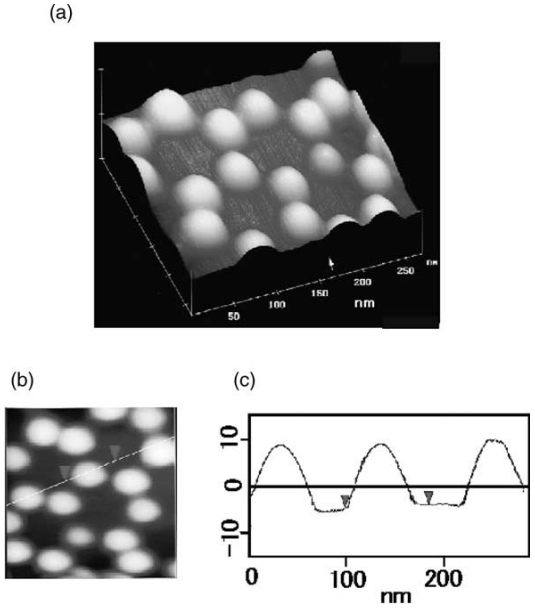

Fig. 2. AFM observations and its height analysis of Al hexagonal dot array on SiO_2, that remained after selective wet chemical etching of porous alumina film.

arose from non-uniformity of anodic oxidation speed with a very thick initial Al thickness of 20 μm. If we use a thinner Al film with a shorter first step anodization time, regularity of nanohole array as well as Al dot array is poor.

Then, we tried to control the size and arrangement of a nanohole array, by making an array of concavities using AFM nanoindentation prior to Al anodic oxidation [15]. As a matter of fact, it turned out that the use of a thin Al film was essential in the control of nanoholes and Al dots by pretexturing techniques using AFM nanoindentation. The fabrication procedure of the nanohole and Al dot array is shown schematically in Fig. 3. We formed an array of concavities at a constant interval from 50 to 150 nm by an AFM nanoindention on the surface of a sputtered Al film with a thickness of 100 nm (Fig. 3a). Next, a nanohole array was formed by the anodic oxidation using 0.15 M oxalic acid at a DC voltage of 30–40 V (Fig. 3b). Finally, the alumina film was selectively etched away. Al dots that existed at an interface between the porous alumina and SiO_2 films then appeared on the surface (Fig. 3c). We used MMAFM of Beeco Corp. equipped with a diamond tip cantilever, which was specially designed for nanoindentation, with a curvature of 10 nm.

At first we examined the effect of the indentation strength on the nanohole arrangement in the case of tetragonal arrays. Tetragonal hole arrays are known to be unstable when they are created by the periodic concavity formed by indentation using a SiC mold prior to anodic oxidation [17,18]. Tetragonal hole arrays tend to rearrange into trigonal ones during growth of nanoholes by anodic oxidation. If Al film thickness is too large, conversion from tetragonal array to trigonal array proceeds. We used anodic voltage between 30 and 40 V; in these conditions, nanohole nearest neighbor distance is between 65 and 90 nm. We observed tetragonal arrays were stable when the Al film thickness was smaller than 0.5 μm. In the following experiments, we used Al films with 0.1 μm thickness.

We examined a dependence of alumina nanohole arrangement on the indentation strength F. When the indentation strength F was lower than 2.0×10^{-5} N, depths of concavities formed by indentation were equivalent or less to the average roughness of the Al film, and the porous alumina film surface morphology did not show any clear periodicity. In fact, the RMS of the 100 nm thick Al film was about 2.0 nm, and the depth of concavity formed by AFM nanoindentation distributed between 1.0 and 2.5 nm. When the indentation strength was increased to 4.0×10^{-5} N, the concavities depth formed by indentation distributed between 15 and 18 nm, and a very clear periodic tetragonal array of nanoholes was formed after anodic oxidation. Scanning speed of nanoindentation is another important factor to form clearly separated nanoholes. When scanning speed was too high, concavities made by nanoindentation were connected each other and finally nanoholes formed by anodic oxidation were connected. We adopted a scanning speed slower than 10 dots/s for nanoindentation experiments with the indentation force of 4.2×10^{-5} N. This rate is relatively very slow, and it takes pretty long time when a large area is nanoindented.

Next we investigated the effect of an indentation interval (d_{int}) on the spatial order of nanoholes

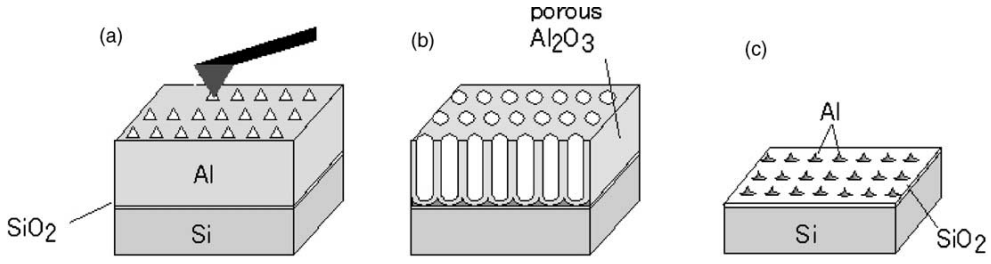

Fig. 3. Schematic diagram of Al nanodot array fabrication procedures.

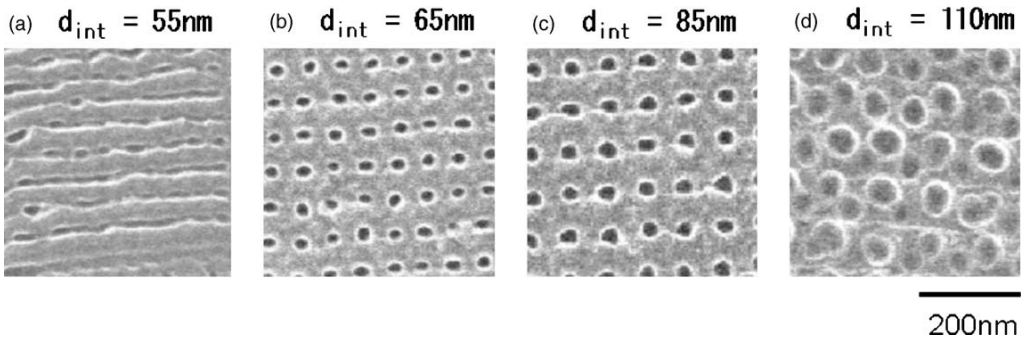

Fig. 4. Porous alumina nanohole array formed by different indentation pitch and the subsequent anodic oxidation. Al surfaces were nanoindented by different intervals from 55 to 110 nm, at the force of 4.16×10^{-5} N, and later they were anodically oxidized at 40 V, 1 min with 0.15 M oxalic acid.

that were formed by anodic oxidation after nanoindentation. Fig. 4 shows SEM micrographs of the surfaces of porous alumina films formed by the anodic oxidation of 40 V at various indentation intervals. At the interval of 55 nm (Fig. 4a), nanoholes were connected to each other. On the other hand, at the interval of 110 nm (Fig. 4d), additional holes were formed randomly between the holes which positions were determined by indentation. The ordered arrays of nanoholes were formed at the intervals of 65 and 80 nm, as shown in Fig. 4b and c. The average interval of holes obtained after anodic oxidation was almost the same as the indentation interval, and there was a linear relationship between them when the indentation interval was smaller than 80 nm. However, in the case of 110 nm interval nanoindentation, the average interval of nanoholes was much smaller than the indented interval. This is due to the formation of additional holes besides those determined by nanoindentation. The spatial order of nanoholes was good when the interval was 65–80 nm, while it got worse when the interval was either smaller or larger than this range. If there is no indentation, an alumina nanohole trigonal array is formed self-organizingly. The nearest neighbor distance of the self-organized nanoholes at 40 V is about 90 nm [8]. If we assume that the cell size is equivalent between triangular and tetragonal arrays, the nearest neighbor nanohole distance in the tetragonal array is estimated to be 78 nm, which is almost the middle of 65 and 85 nm. So we can conclude that if the cell size of the nanoholes differs too much from that of the self-organization condition, the order of the nanohole arrangement becomes poor.

We attempted to form tetragonal as well as trigonal Al dot arrays by selective wet chemical etching of porous alumina films. SEM plan-view images and AFM images of the trigonal as well as tetragonal Al dots at the 65 nm indentation interval are shown in Fig. 5. The voltage for anodic oxidation was 30 V. The height and the nearest neighbor distance of the Al dots are 15 and 45 nm for trigonal array, and 20 and 65 nm for tetragonal array, respectively.

We further evaluated electron transport property by attaching electrodes around Al nanodot array. Tetragonal Al dot array was formed by anodic oxidation at 40 V and indentation interval with 65 nm. Two tungsten electrodes were formed using focused ion beam induced deposition as shown schematically in the inset of Fig. 6. The distance of the gap between electrodes was about 1.5 μm and the width of each electrodes was 1.0 μm, thus 23×15 dots array existed between the electrodes. A current–voltage characteristic of Al dot array are shown in Fig. 6. There is a non-linear current–voltage characteristics at room temperature (Fig. 6a). This is considered to come from tunneling current between the dots, in which alumina barrier exited in between dots. When temperature was lowered to 4.2 K, a suppression of the current near zero bias that was supposed to

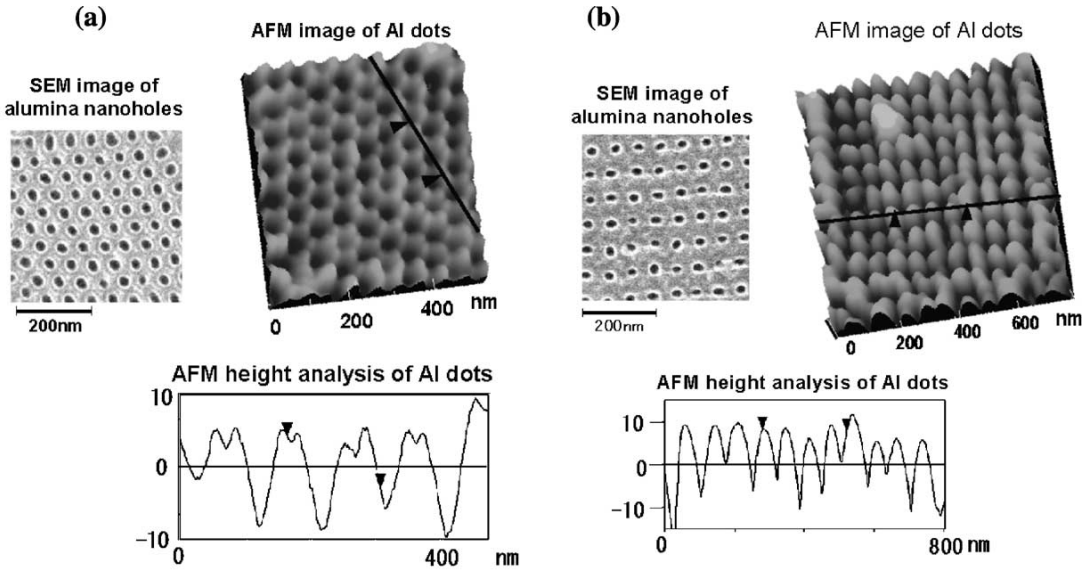

Fig. 5. Trigonal (a) and tetragonal array (b) of nanoholes and Al dots formed by AFM nanoindentation and anodic oxidation. Interval of nanoindentation was 65 nm, and anodic voltage was 30 V. SEM plan view micrographs of the nanohole, AFM image of Al dots after selective wet chemical etching, and its height analysis are shown.

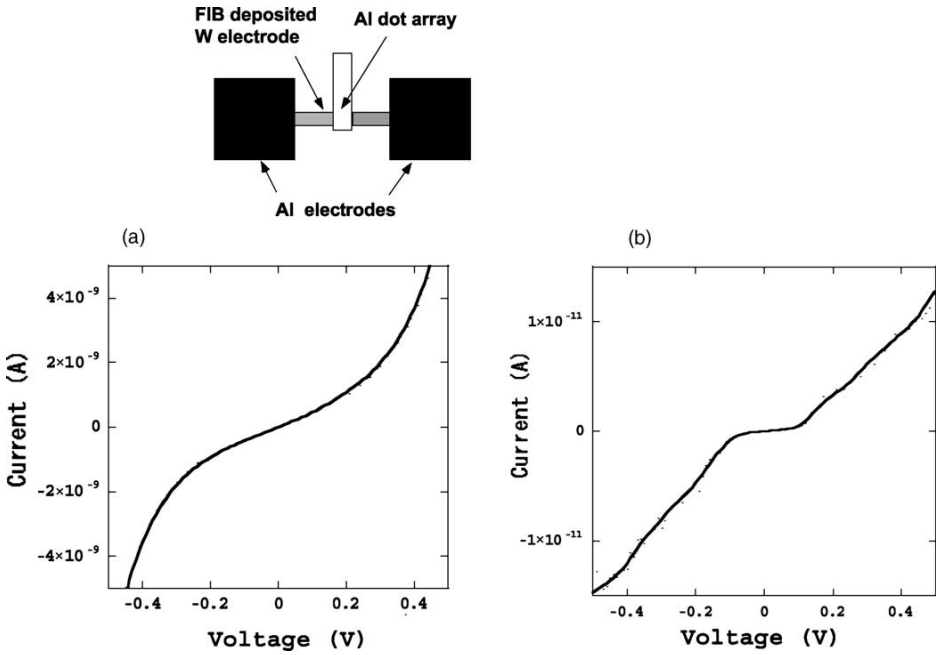

Fig. 6. Current–voltage characteristics of 23×15 Al dot array measured at (a) 298 and (b) 4.2 K.

come from the Coulomb blockade due to single electron charging effect was observed. The off-set voltage (V_{off}) was 0.13 V. If a current passes along the most conductive path with N-junctions of Al dots, V_{off} is approximately equal to $N(e/2C)$ [19], and C is estimated to be 2.4×10^{-17} F assuming that N is 23. The control of tunneling gap between Al dots is not so easy since anodic oxidation still continues even after Al film was broken up to islands. In other samples that were formed almost in the same way, some were completely insulating due to too large gap between Al dots, and for others cases, Al dots were connected and linear current–voltage characteristics were observed, and further, we observed some kind of hopping conductions in some other sample. Further delicate control of the gap between dots would be needed to observe tunneling effect more stably.

3. Conclusions

Porous Al film was formed on SiO_2/Si substrate, and after completion of anodic oxidation of Al film, hexagonal Al dot array was confirmed by cross-sectional SEM and TEM observations. By the use of AFM nanoindentation prior to anodic oxidation, tetragonal array of Al nanodot that could not be realized by self-organization was formed. The ordered array of alumina nanohole or Al nanodot could be obtained at the indentation interval, which was close to that of the self-organization condition at a given anodic voltage. The results suggest that adjusting the anodic voltage against to the indentation interval can form Al dot array with a desired geometry. Furthermore, we observed a non-linear current–voltage characteristics in the Al dots array at 4.2 K, which strongly suggests Coulomb blockade between dots. These results strongly suggest a high potentiality of porous alumina based nanofabrication to various nanoelectron devices.

References

[1] F. Keller, M.S. Hunter, D. Robinson, J. Electrochem. Soc. 100 (1953) 411.
[2] J.P. O'Sullivan, G.C. Wood, Proc. Roy. Soc. London A 317 (1970) 511.
[3] C.G. Granqvist, A. Anderson, O. Hundrei, Appl. Phys. Lett. 35 (1979) 268.
[4] H.L. Hornyak, C.J. Patrissi, C.R. Martin, J. Phys. Chem. B 101 (1997) 1548.
[5] D. Routkevitch, T. Bigioni, M. Moskovits, J.M. Xu, J. Phys. Chem. 100 (1996) 14037.
[6] D. Routkevitch, A.A. Tager, J. Haruyama, D. Almawlawi, M. Moskovits, J.M. Xu, IEEE Trans. Electron Devices 43 (1996) 1646.
[7] H. Masuda, K. Fukuda, Science 268 (1995) 146.
[8] S. Shingubara, O. Okino, Y. Sayama, H. Sakaue, T. Takahagi, Jpn. J. Appl. Phys. 36 (1997) 7791.
[9] H. Masuda, F. Kasegawa, S. Ono, J. Electrochem. Soc. 144 (1997) L127.
[10] H. Masuda, K. Yada, A. Osaka, Jpn. J. Appl. Phys. 37 (1998) L1340.
[11] S. Shingubara, O. Okino, H. Sakaue, T. Takahagi, Solid State Electron. 43 (1999) 1143.
[12] S. Shingubara, O. Okino, H. Sakaue, T. Takahagi, J. Vac. Sci. Technol. B 19 (2001) 1901.
[13] Y. Murakami, S. Shingubara, H. Sakaue, T. Takahagi, Digest papers of Microproc. Nanotechnol. 2000 (2000) 178.
[14] S. Shingubara, Y. Murakami, H. Sakaue, T. Takahagi, Jpn. J. Appl. Phys. 41 (2002) L340.
[15] S. Shingubara, Y. Murakami, H. Sakaue, T. Takahagi, Mat. Res. Soc. Symp. Proc. 705 (2002) 133.
[16] I. Amlani, A.O. Orlov, R.K. Kummamuru, Appl. Phys. Lett. 77 (2000) 738.
[17] H. Masuda, H. Yamada, M. Satoh, H. Asoh, Appl. Phys. Lett. 71 (1997) 2770.
[18] H. Asoh, K. Nishio, M. Nakao, T. Tamamura, H. Masuda, J. Electrochem. Soc. 128 (2001) B152.
[19] H. Grabert, M.H. Devoret (Eds.), Single Charge Tunneling—Coulomb Blockade Phenomena in Nanostructures, Nato ASI Series, Prenum Publishing, New York, 1992 (Chapter 7).